Damage Tolerant ECC for Integrity of Structures Under Extreme Loads

Author:

Victor C. Li, Department of Civil and Environmental Engineering, University of Michigan, Ann Arbor, MI 48109-2125, vcli@umich.edu

ABSTRACT

Engineered Cementitious Composite (ECC), a highly ductile concrete material with a tensile strain capacity several hundred times that of normal concrete, is establishing itself as a new construction material that can lead to substantial improvements in structural performance. A number of full-scale structural applications of ECC in the US and in Japan indicate that various unique characteristics of ECC, including its tensile ductility and self-controlled crack width, can be exploited to enhance structural safety and durability.

This paper reviews the unique characteristics of ECC important to structural applications. Specifically, the tensile, shear and flexural ductility of ECC, and the distinctive nature of microcracking during inelastic deformation will be discussed in the context of structural member damage tolerance and energy absorption capacity under earthquake loading. The ductility of ECC will also be discussed in the context of resistance to penetration and fragmentation in protective structures subjected to impact loads. Finally, it is suggested that the ability to systematically tailor ECC for strength, ductility and stiffness, as well as other material characteristics provides expanded design space for structural member performance optimization much beyond that with normal reinforced concrete. This paper draws heavily from that contained in a book chapter on ECC by the author [Li, 2008] and from an article on impact resistance design of ECC [Yang et al, 2007].

INTRODUCTION

ECC is a family of concrete materials with a range of tensile strength, ductility and stiffness (Table 1) that can be engineered to meet the demands of a particular structural member. ECC is often regarded as belonging to the class of high performance fiber reinforced concrete (HPFRCC) due to its strain-hardening response after first cracking under uniaxial tensile loading. ECC stands out in its ability to tolerate tensile strain several hundred times that of normal concrete and ordinary fiber reinforced concrete prior to failure. This high tensile ductility makes ECC particularly attractive to structures that may be exposed to extreme loading such as earthquake or impact loading.

The unique tensile ductility of ECC is illustrated in Figure 1 which shows a uniaxial tensile stress-strain curve with a strain capacity of 5%. This metal-like behavior shows a characteristic "yield point" at the end of the elastic stage when the first microcrack appears on the specimen.

The tensile strain-hardening response is accompanied by multiple microcracking as opposed to localized crack opening commonly observed in concrete or fiber reinforced concrete (FRC). Final failure of the specimen occurs when one of the multiple cracks forms a fracture plane. Beyond this peak load, ECC is no different than normal FRC, showing a tension-softening behavior. The high material ductility is of value in enhancing structural load and deformation capacity as well as energy absorption. Due to its damage-tolerant characteristic, ECC offers structural safety improvements, while minimizing repair cost subsequent to extreme loading.

Compressive Strength (MPa)	First Crack Strength (MPa)	Tensile Strength (MPa)	Tensile Strain (%)	Young's Modulus (GPa)	Flexural Strength (MPa)	Density (g/cc)
20 – 95	3 – 7	4 – 12	1 – 8	14 – 34	10 – 30	0.95 – 2.3

TABLE 1 - MAJOR PHYSICAL PROPERTIES OF ECC

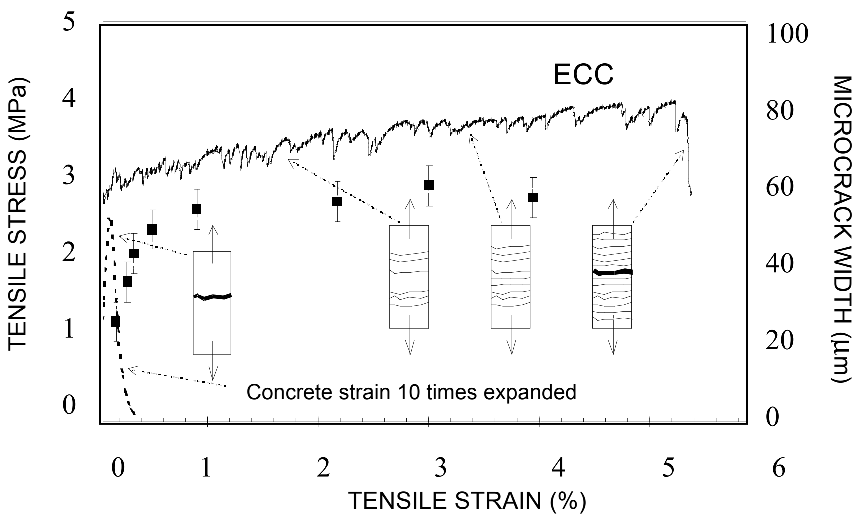

FIGURE 1 - A TYPICAL TENSILE STRESS-STRAIN RELATION OF AN ECC

The formation of multiple microcracking is necessary to achieve high composite tensile ductility. Between first cracking strain (about 0.01%) and 1% strain, the microcrack opening increases from zero to about 60 µm. Further loading beyond 1% causes more multiple cracks to form, but with no additional crack opening beyond the steady state value of 60 µm (Figure 1). This unique characteristic is critically important for durability [Şahmaran and Li, 2009] of both material and structure. Unlike concrete or FRC, the steady state crack width is an intrinsic material property, independent of loading (tension, bending or shear), structure size and geometry, and steel reinforcement type and amount. This observation has important implications in service life, maximum member size, economics, and architectural aesthetics. In short, where steel reinforcement is used to control crack width in concrete, such steel reinforcement can be eliminated in ECC. By suppressing cracks with large crack width even in the presence of large imposed structural deformations, ECC can offer structural durability improvements in addition to water tightness and other serviceability enhancements.

The compressive properties of ECC are not significantly different from normal to high strength concrete. Compressive strength of ECC ranges from 30MPa to 90MPa (with special versions such as ultra lightweight ECC falling outside this range). The elastic modulus (around 20-25 GPa) of ECC is typically lower than that of concrete due to the absence of coarse aggregates. The compressive strain capacity of ECC is slightly higher, around 0.45-0.65%. The post-peak behavior of ECC under compression tends to descend more gently than high strength concrete, accompanied by a gradual bulging of the specimen rather than explosive crushing failure.

In recent years, a number of full-scale applications of ECC have been carried out in various countries. Foremost amongst these is the use of ECC in precast R/ECC coupling beams in the core of three high rises in Japan [Maruta et al, 2005; Kunieda and Rokugo, 2006]. This application exploits the high energy absorption capability of R/ECC to aid in seismic resistance of these tall buildings. Other notable applications include cast in place ECC link slabs on bridge decks [Kim et al, 2004; Lepech and Li, 2005] in the US and Italy, a composite ECC/Steel bridge deck in Japan [Mitamura et al, 2005], sprayed ECC tunnel linings in South Korea, repair of the Mitaka Dam in Japan [Kojima et al, 2004], irrigation channel repairs in Japan [Kunieda and Rokugo, 2006] and in the US [Li et al, 2009], and prototype pipe extrusion in Australia. Several projects in the housing and in the energy industries employing ECC are in various planning stages. Despite the evolving development of ECC material and field applications, a great deal of research and experimentation remains. Indeed, the transformation of brittle concrete to ductile ECC offers enormous opportunities in structural innovations not possible previously.

MIXTURE PROPORTIONING AND MATERIAL PROCESSING

Table 2 gives a typical mix design of ECC (ECC-M45) with self-consolidating casting properties. All proportions are given with materials in the dry state.

Mix Designation	Cement	Fly Ash	Sand	Water	HRWR*	Fiber (Vol %)
M45	1.0	1.2	0.8	0.56	0.012	0.02

*High Range Water Reducer

TABLE 2 - A TYPICAL ECC (ECC-M45) MIX DESIGN BY WEIGHT

Adaptations of this reference mix have been used in various construction projects. Full-scale production of ECC was carried out in Japan [Kunieda and Rokugo, 2006], and in the US [Lepech and Li, 2008]. Experience in concrete ready-mix plants suggests the following raw material charging sequence:

Activity No.	Activity	Elapsed Time (min)
1	Charge all sand	2
2	Charge approximately 90-95% of mixing water, all HRWR, all hydration stabilizer	2
3	Charge all fly ash	2
4	Charage all cement	2
5	Charge remaining mixing water to wash drum fins	4
6	Mix at high RPM for 5 minutes or until material is homogenous	5
7	Charge fibers	2
8	Mix at high RPM for 5 minutes or until material is homogenoug	5
	Total	24

TABLE 3 - MATERIAL CHARGING SEQUENCE INTO READY-MIX TRUCKS

FIGURE 2 - READY-MIX TRUCK MIXING AND SELF-CONSOLIDATING CASTING OF ECC

BEHAVIOR OF ECC STRUCTURAL ELEMENTS

A variety of experiments have been performed to assess the performance of ECC at the structural element level for seismic applications (Table 4). These experiments provide insights into how unique ECC material properties elevate the structural performance.

* steel reinforcement unless specified

Structural Element Type	**Type of Loading (type of reinforcement)***	**Reference**
Flexural elements	Reversed cyclic Reversed cyclic (CFRP)	[Fischer and Li, 2002] [Fischer and Li, 2003]
Shear beam elements	Reversed cyclic	[Kanda et al, 1998], [Fukuyama et al, 2000]
Column elements	Reversed cyclic	[Fukuyama et al, 2000]
Wall elements	Repeated shear Reversed cyclic	[Kanda et al, 1998] [Kesner and Billington, 2005] [Fukuyama et al, 2006]
Frames	Reversed cyclic (steel & CFRP)	[Fischer and Li, 2003]

TABLE 4 - VARIOUS R/ECC STRUCTURAL ELEMENTS PREVIOUSLY STUDIED

Structural Response of R/ECC Elements Under Reverse Cyclic Loading

Flexural Elements: Fischer and Li [2002] studied the behavior of R/ECC flexural elements under reversed cyclic loading. Figure 3 shows the hysteretic response for the R/ECC and the R/C control column specimens. A significantly fuller hysteretic loop with larger energy dissipation was achieved by the R/ECC beam despite the fact that no shear stirrups were used. The damage experienced by these elements at 10% interstory drift is compared in Figure 4. Even at this high drift level, no spalling of the ECC was observed. In contrast, the R/C column lost all concrete cover near the fixed end subsequent to bond splitting and spalling. Clearly, the R/ECC element demonstrated significant damage tolerance under severe loading.

Shear Elements: Fukuyama et al [2000] studied the behavior of R/ECC shear elements under reversed cyclic loading. Again, the hysteretic loops for R/ECC showed much greater stability and ability to dissipate energy (Figure 5). The R/C specimen suffered extensive bond splitting and loss of cover, accompanied by large diagonal cracks. In contrast, the damage experienced by the R/ECC shear element was significantly lower (Figure 6). No bond splitting and cover loss was observed and microcracks continued to carry loads up to 5% rad deflection angle.

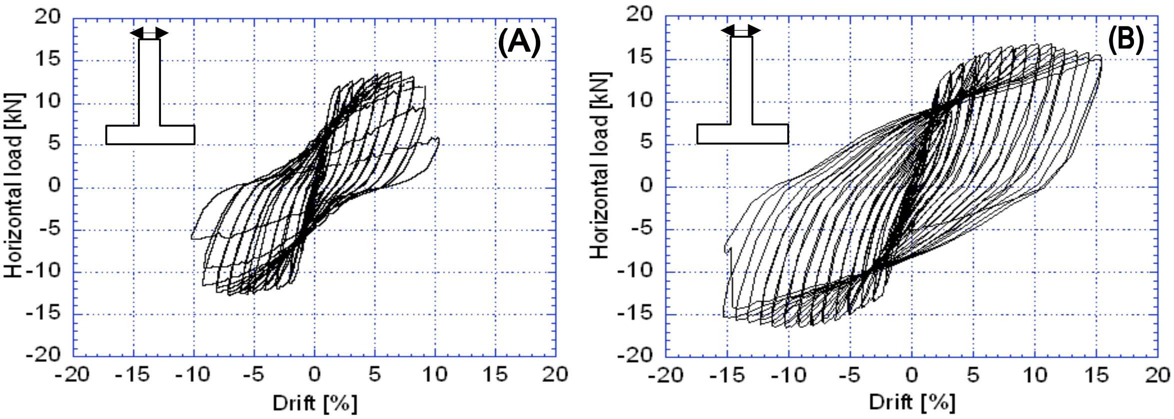

FIGURE 3 - HYSTERETIC BEHAVIOR OF FLEXURAL MEMBERS UNDER REVERSED CYCLIC LOADING FOR (A) R/C WITH STIRRUPS, AND (B) R/ECC WITHOUT STIRRUPS [FISCHER AND LI, 2006].

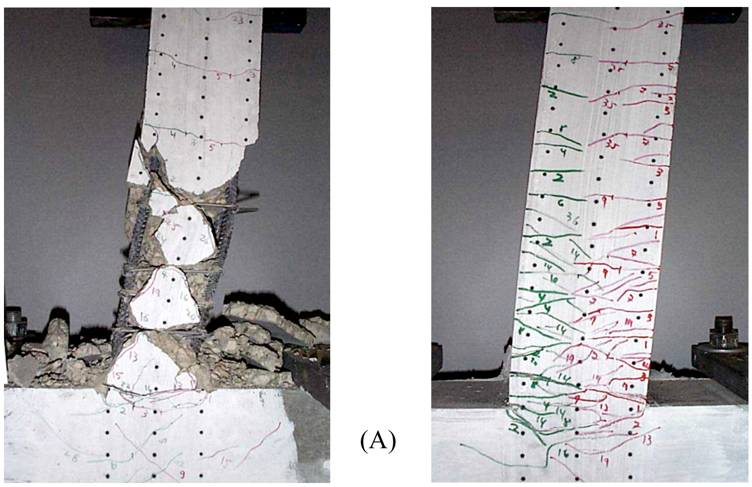

(A) (B)

FIGURE 4 - DAMAGE BEHAVIOR OF (A) R/C WITH STIRRUPS AND (B) R/ECC WITHOUT STIRRUPS, SHOWN AT 10% DRIFT [FISCHER AND LI, 2006].

Column Element: The response of R/ECC and R/C columns under fully reversed cyclic loading was studied by Fukuyama et al [2000]. These columns were tested under anti-symmetrical moment condition. The axial force applied to the column is 20% of the axial compressive strength of the column, calculated without the contribution of the steel reinforcements. The hysteretic behavior in terms of stability and energy dissipation was improved in R/ECC column over R/C column in a similar manner as for flexural and shear elements. Large bond splitting cracks were observed in the R/C column which failed by shear without yielding of the longitudinal reinforcements. Subsequently, the resistant shear force in the envelope curve of shear force – deflection angle relationship decreased with increase of deflection angle. On the other hand, the R/ECC column did not fail by shear or bond splitting. Instead, it maintained a ductile response up to the end of the test with fine cracks revealed on the specimen surface.

Wall Panel Element: Wall panel elements were studied by Kesner and Billington [2005] under fully reversed cyclic loading. These tests confirmed that the R/ECC wall panels outperformed the R/C wall panels in hysteretic loop stability, peak load, and energy dissipation. The structural element experimental testing results briefly summarized above share the common features of enhanced element load and deformation capacity, hysteretic loop stability, and energy dissipation. Further, structural damage is limited to microcracking while large fractures in the form of bond splitting and spalling are suppressed.

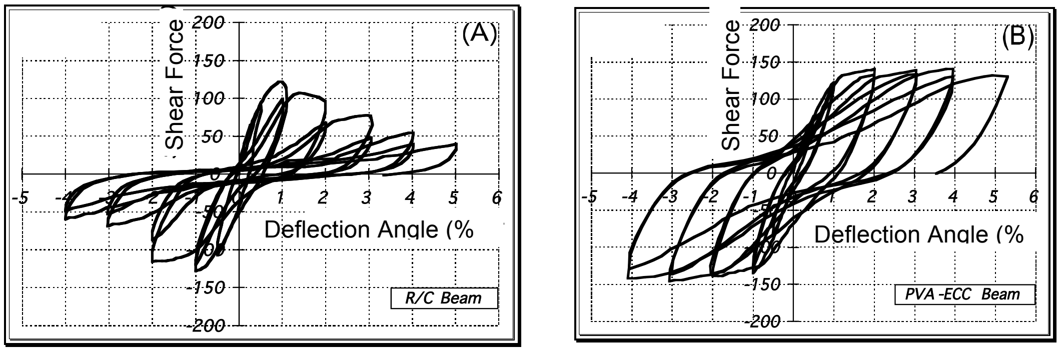

FIGURE 5 - HYSTERETIC LOOPS FOR SHEAR BEAMS UNDER FULLY REVERSED CYCLIC LOADING FOR (A) R/C, AND (B) R/ECC [FUKUYAMA ET AL, 2000].

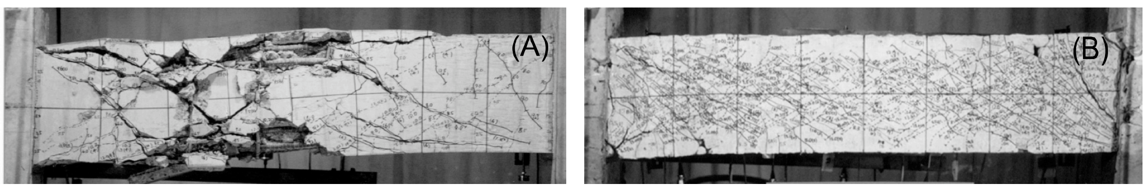

FIGURE 6 - DAMAGE PATTERN IN OHNO SHEAR BEAMS (A) R/C, AND (B) R/ECC [FUKUYAMA ET AL, 2000].

Insights from R/ECC element response

From the above cited studies, it emerges that ECC has at least the following advantages when properly deployed in structural members under seismic loading [Li, 2008]:

- Potential for reduction or elimination of shear reinforcement
- Damage tolerance and minimized repair needs
- Compatible deformation between ECC and reinforcement
- Tight crack width control and elimination of crack control reinforcement
- Transforming material ductility into structural strength

R/ECC is a composite with elastic-plastic steel reinforcing elastic-strain-hardening ECC. With large deformation capacity for both, they deform compatibly even at large imposed drifts, minimizing steel/ECC interface shear stress and maximizing plastic energy dissipation of steel.

IMPACT BEHAVIOR OF ECC ELEMENTS

Rate Dependent Property of ECC

Concrete is known to exhibit loading rate dependencies, including higher tensile and compressive strength accompanied by higher brittleness at higher loading rates [Malvar and Ross, 1998]. Brittle failures (e.g. cracking, spalling, and fragmentation) of concrete are often observed in R/C structures when subjected to impact/blast, and can lead to severe loss of structural integrity [Clifton, 1984].

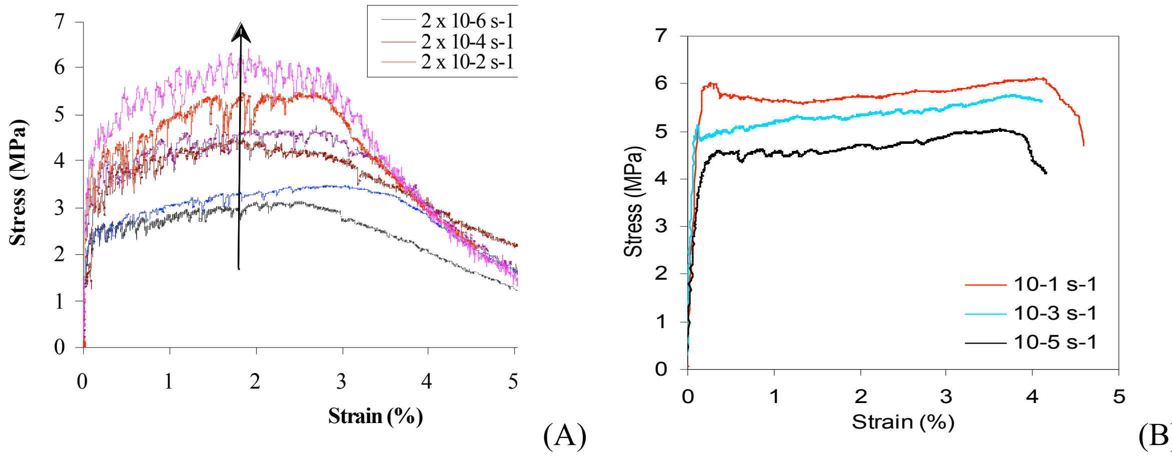

FIGURE 7 - TENSILE STRESS-STRAIN CURVE OF (A) HYBRID-FIBER ECC [ZHANG ET AL, 2005] AND (B) HVFA-ECC [YANG ET AL, 2007] UNDER VARIOUS LOADING RATES

Yang et al [2007] studied impact behavior of ECC and found that with proper micromechanical engineering, it is possible to maintain the tensile ductility of ECC at low velocity impact loading rates. Figure 7 shows the tensile stress-strain behavior of a hybrid-fiber (steel and PE) [Zhang et al, 2005] ECC subjected to six different loading rates. The test results show that there is a substantial increase in the ultimate tensile strength from 3.1 MPa to 6 MPa with increasing strain rate, while the average strain capacity ranges between 2.7 to 3.3% without a clear indication of rate sensitivity. Figure 7b shows the tensile stress-strain curve of another version (HVFA ECC) of ECC containing PVA fibers and high volume fly ash (with 75% of cement replaced by class F fly ash), at three different loading rates. Again, it was found that tensile strength increases with strain rate while tensile strain capacity remains approximately constant (~3.9%).

Impact Resistance of Simple ECC and R/ECC Structural Elements

Impact resistance of R/ECC panel: Drop weight impact tests were conducted on R/ECC (f'_c = 74MPa), R/FRC (f'_c = 75MPa) as well as normal strength R/C (f'_c = 40MPa) panels [21]. In this series of test, hybrid-fiber ECC was used to construct the R/ECC. All panels measuring 2m x 1m x 0.1m (length x width x thickness) were reinforced orthogonally with 8 mm diameter mild steel bars spaced at 150 mm center to centre (ρ = 0.6%). For each impact, a 45 kg hammer with a hemispherical tip of diameter 95 mm was raised to a height of 4 m and allowed to drop freely under its own weight onto the centre of the specimen. The same drop height of 4 m was maintained for each impact. For each specimen, resistances under multiple impacts were monitored repeatedly until the panels were totally perforated.

For R/C and R/FRC panels, multiple impact tests were performed until the panel was perforated by the drop hammer, while the test on R/ECC panel were aborted after the tenth impact in view of the minor damage caused. Generally, R/ECC panels were found to show significantly improved impact and fragmentation resistance. On the impact side, the R/C and R/FRC panels were perforated after the 3rd and 7th impacts, respectively. Only minor indentation with no debris was observed in the R/ECC panel after the 10th impact. The differences in damage behavior between the three specimens on the distal face are dramatic. In the case of R/C, serious scabbing and large debris after the 2nd impact results (Figure 9a). R/FRC panel showed improved impact resistance (Figure 9b) with less fragmentation. The R/ECC panel showed no fragmentation with only minor damage (Figure 9c), where the micro-cracks were highlighted using a thick marker.

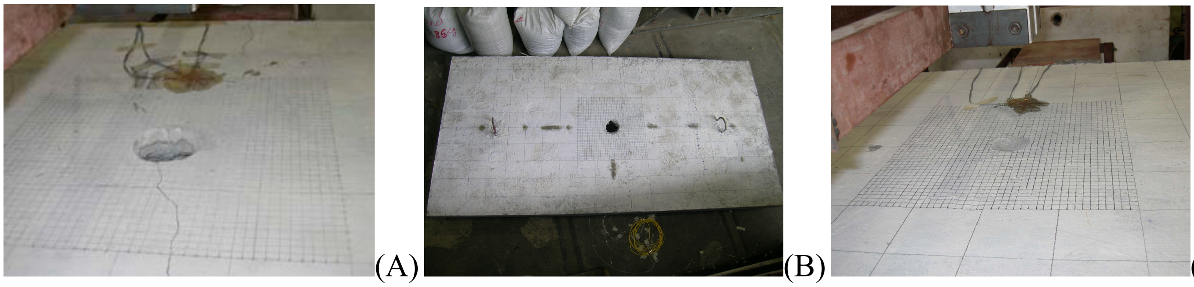

(A) (B) (C)

FIGURE 8 - DAMAGE ON THE IMPACT FACE OF (A) R/C PANEL AFTER 3RD IMPACT, (B) R/FRC PANEL AFTER 7TH IMPACT, AND (C) R/ECC PANEL AFTER 10TH IMPACT [ZHANG ET AL, 2005]

(A) (B) (C)

FIGURE 9 - DAMAGE ON DISTAL FACE OF (A) R/C PANEL AFTER 2ND IMPACT, (B) R/FRC PANEL AFTER THE 7TH IMPACT, AND (C) R/ECC PANEL AFTER 10TH IMPACT [ZHANG ET AL, 2005]

After each impact test, the damage level was evaluated and characterized. The penetration depth, crater diameter, and impact force sustained are shown in Figure 10. The R/ECC panel shows significant impact resistance compared with R/C and R/FRC.

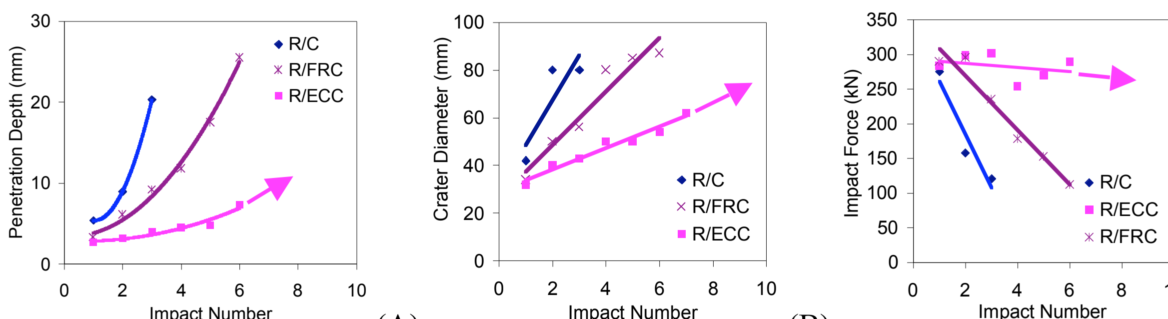

(A) (B) (C)

FIGURE 10 - (A) INDENTATION DEPTH, (B) CRATER SIZE, AND (C) LOAD CELL PEAK IMPACT FORCE AGAINST NUMBER OF IMPACTS [ZHANG ET AL, 2005]

Impact Resistance of ECC Circular Plate: Circular plate specimens of a high flyash content ECC (f'_c = 39MPa) and mortar (f_{cube} = 35MPa) were tested under drop weigh impacts [Yang et al, 2007]. The plates (diameter = 350mm, thickness = 13mm) were supported along the perimeter at a span of 330mm. The striking mass was a 35mm, 977 gram steel cylinder. At each test the striking mass was dropped from various heights of 50, 75, 100, 125, and 140 cm with corresponding strain rates of 0.23, 1.11, 2.05, 3.53 and 4.28 s^{-1} (striking velocities ranged from

1.2 to 5 m/sec). After each drop the plates were visually examined to determine viability of the next drop.

The control mortar plate withstood the first 50-cm drop but failed under the 2nd impact of 75-cm drop with severe cracking and fragmentation (Figure 11a), whereas the test on ECC plates were aborted after a series of drops (two dropping series of 50, 75, 100, 125 and 140 cm, total 10 impacts) with only minor damage caused. Again, ECC plates showed superior impact resistance when compared with mortar specimens. While the control mortar plate withstood only a single impact, ECC plates withstood all impact levels (i.e. from all drop heights) without significant damage after the first test series (five drops). The ECC specimens remained without major damage and showed significant load carrying capacity in the second series of drops. Only fine multiple microcracks were found on the backside of the plates as shown in Figure 11b.

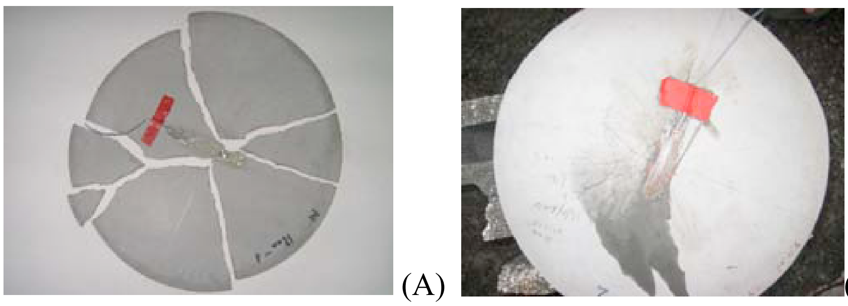

(A) (B)

FIGURE 11- (A) MORTAR PLATE AFTER THE 2ND IMPACT (CRACKING & FRAGMENTATION) AND (B) BACK SIDE OF ECC PLATE AFTER 10 IMPACTS (FINE CRACKS ONLY) [YANG ET AL, 2007]

CONCLUDING REMARKS

As a structural material, ECC maintains all the advantages of concrete, but overcomes its familiar brittleness in tension. Experimental studies confirm that ECC is highly damage tolerant under extreme loading, including reverse cyclic loading and low velocity impact. Hence it is expected that ECC will contribute to enhancing structural safety while minimizing repair requirements subsequent to an extreme loading event. Apart from resisting earthquake loads, ECC will likely perform well under hurricane loading, although more studies need to be conducted to confirm this. Research on high velocity impact resistant ECC is now underway at the University of Michigan.

The moderate fiber content (2% or less by volume) makes ECC easily adaptable to construction project execution in the field or to precast plant structural element production. Indeed, ECC has demonstrated to possess flexibility in processing routes, including on-site self-consolidating casting, and spraying, as well as off-site precasting and extrusion. Maintaining a moderately low fiber content is obviously important also for economic viability for infrastructure applications.

REFERENCES

1. Li, V.C., "Engineered Cementitious Composites – Material, Structural, and Durability Performance," in *Concrete Construction Engineering Handbook*, Chapter 24, Ed. E. Nawy, CRC Press, 2008.

2. Yang, E.H., V.C. Li, A.N. Dancygier, D. Yankelevsky, A. Katz, and A. Bentur, "Impact Resistance of Engineered

Cementitious Composites," in CD: International Symposium on Interaction of the Effects of Munitions with Structures (ISIEMS) 12.1, published by the Defense Threat Reduction Agency, 2007.

3. Şahmaran, M. and V.C. Li, "Engineered Cementitious Composites: An Innovative Concrete for Durable Structure," this volume, Proc., ASCE Structures Congress, Austin, Texas, April-May, 2009.

4. Maruta, M., Kanda T., Nagai S. and Yamamoto, Y. 2005. New high-rise RC structure using pre-cast ECC coupling beam. *Concrete Journal* 43(11):18-26.

5. Kunieda, M. and Rokugo, K. 2006. Recent progress on HPFRCC in Japan – Required performance and applications. *J. Advanced Concrete Technology* 4(1):19-33, Japan Concrete Institute.

6. Kim, Y.Y., Fischer, G. and Li, V.C. 2004. Performance of bridge deck link slabs designed with ductile ECC. *ACI Structural J.* 101(6):792-801.

7. Lepech, M.D. and Li, V.C. 2005. Design and field demonstration of ECC link slabs for jointless bridge decks. *ConMat'05*, Vancouver, Canada, CD-documents/1-05/SS-GF-05_FP.pdf.

8. Mitamura, H., Sakata, N., Shakushiro, K., Suda, K. and Hiraishi, T. 2005. Application of overlay reinforcement method on steel deck utilizing ECC – Mihara Bridge. *Bridge and Foundation Engrg.* 39(8):88-91.

9. Kojima, S., Sakat, N., Kanda, T. and Hiraishi, T. 2004. Application of direct sprayed ECC for retrofitting dam structure surface – application for Mitaka-Dam. *Concrete Journal* 42(5):35-39.

10. Li, V.C., G. Fischer, and M. Lepech 2009. "Shotcreting with ECC," in Proc., Spritzbeton-Tagung, Austria, Jan., 2009.

11. Lepech, M.D., and V.C. Li, "Large Scale Processing of Engineered Cementitious Composites," *ACI Materials J.*, 105(4) 358-366, 2008.

12. Fischer, G. and Li, V.C. 2002. Effect of matrix ductility on deformation behavior of steel reinforced ECC flexural members under reversed cyclic loading conditions. *ACI Structural J.* 99 (6):781-790.

13. Fischer, G., and Li, V.C. 2003. Deformation Behavior of Fiber-Reinforced Polymer Reinforced Engineered Cementitious Composite (ECC) Flexural Members under Reversed Cyclic Loading Conditions. *ACI Structural J.*, 100(1):25-35.

14. Kanda, T., Watanabe, S. and Li, V.C. 1998. Application of pseudo strain hardening cementitious composites to shear resistant structural elements. In *Fracture Mechanics of Concrete Structures Proc. FRAMCOS-3*, 1477-1490.

15. Fukuyama, H., Matzuzaki, Y., Sato, Y., Iso, M. and Suwada, H. 2000. Structural performance of engineered cementitious composite elements. *Composite and Hybrid Structures, 6th ASCCS Int'l Conf. on Steel-Concrete Composite Structures,* pp. 969-976.

16. Kesner, K.E. and Billington, S.L. 2005. Investigation of infill panels made from engineered cementitious composites for seismic strengthening and retrofit. *ASCE J. Struc. Engrg* 131(11): 712-1720.

17. Fukuyama, H., Suwada, H. and Mukai, T. 2006. Test on High-Performance Wall Elements with HPFRCC, In *Proc., Int'l RILEM Workshop HPFRCC in Structural Applications*, Eds. Fischer, G., and V.C. Li, published by RILEM SARL, pp. 365-374.

18. Fischer, G., and Li, V.C. 2003. Intrinsic Response Control of Moment Resisting Frames Utilizing Advanced Composite Materials & Structural Elements. *ACI Structural J.,* 100(2):166-176.

19. Malvar, L.J., and C.A. Ross, *Review of Strain Rate Effects for Concrete in Tension.* ACI Materials Journal, 1998. 95(6): p. 735-739.

20. Clifton, J.R., *Penetration Resistance of Concrete - A Review*, in *National Bureau of Standards, special publication 480-45*. 1984: Washington DC.

21. Zhang, J., M. Maalej, S.T. Quek, and Y.Y. Teo. *Drop Weight Impact on Hybrid-fiber ECC Blast/Shelter Panels*, in *Proceedings of Construction Materials*. 2005. Vancouver, Canada.